

# Methyl Group Dynamics in Poly(vinyl methyl ether). A Rotation Rate Distribution Model

A. Chahid, A. Alegría, and J. Colmenero\*

Departamento de Física de Materiales, Facultad de Química, Universidad del País Vasco (UPV/EHU), Apartado 1072, 20080 San Sebastián, Spain

Received January 27, 1994; Revised Manuscript Received March 17, 1994\*

**ABSTRACT:** The dynamics of the methyl side group in poly(vinyl methyl ether) (PVME) is investigated by means of time-of-flight quasi-elastic neutron scattering in the time range between  $10^{-11}$  and  $10^{-13}$  s. The quasi-elastic region of the experimental data is analyzed by using two alternative different models. One of them assumes that there exist two different families of  $\text{CH}_3$  in PVME moving at different rates and with a population which depends on temperature. The other model assumes a single type of  $\text{CH}_3$  groups but considers the existence of a random distribution of jumping rates for the methyl group rotation. Both models allow a good description of the experimental behavior. However, whereas the former results in a peculiar behavior of the model parameters, the latter leads to a simple and physical picture of the methyl group dynamics. In particular, a Gaussian distribution of the energy barriers for the  $\text{CH}_3$  rotational jumps which is centered at  $8.4 \text{ kJ mol}^{-1}$  and has a distribution width of  $\pm 0.8 \text{ kJ mol}^{-1}$  is found to be the origin of the distribution of jumping rates. Within the experimental uncertainties, the distribution of energy barriers does not change with temperature around the glass transition.

## 1. Introduction

Side-group motions in polymers have been the subject of numerous investigations by several techniques such as nuclear magnetic resonance, mechanical and dielectric relaxation, and neutron scattering (NS).<sup>1</sup> Among the different side groups investigated the methyl group appears to perform very fast motions which can be related to very low temperature relaxation peaks in mechanical spectroscopy. This fact is associated with the relatively low barriers of rotation of the methyl groups. The high frequencies corresponding to the NS experiments together with the high incoherent cross section of the protons make the NS technique very adequate for the study of the methyl group dynamics. Moreover, NS, when compared with relaxation techniques, presents the particular advantage that it allows us to get information not only about the dynamics of the motion but also about its particular geometry.<sup>2</sup>

Methyl side groups have been studied by means of NS techniques in a wide range of polymers such as poly(methyl methacrylate) (PMMA), poly(propylene oxide) (PPO), polypropylene (PP), etc.,<sup>3-5</sup> and also in polymers blends.<sup>6</sup> From these studies it turns out that the dynamics of this side group is sensitive to the chemical nature of the main chain as well as to its configuration. Two main types of motion have been reported for this side group unit. When the  $\text{CH}_3$  group is directly linked to the main chain, it appears that the  $\text{CH}_3$  performs a torsional motion that can be mainly detected as an inelastic peak in the NS spectra. On the other hand, when the  $\text{CH}_3$  group is a part of an ester side group, the energy barrier is very low and the hindered rotation of the methyl group protons, which is clearly evidenced as the broadening of the elastic peak in the NS spectra, appears to be the main dynamical process. Therefore, in order to study this last motion, it is necessary to use quasi-elastic neutron scattering (QENS) techniques. The geometry of the motion usually considered for the  $\text{CH}_3$  dynamics is the rotation of the protons among three positions.<sup>4-6</sup> This model has been successfully applied in order to give account of the methyl dynamics in molecular crystals.<sup>2</sup> However, when it is applied to

explain the  $\text{CH}_3$  dynamics in polymers, several peculiar results are obtained. First of all, the experimental elastic incoherent structure factor (EISF), which is calculated from the spectra as the ratio of the elastic intensity to the total scattered intensity, is higher than the one deduced from the model and depends on temperature.<sup>4-6</sup> This fact has led several authors to assume that in the case of the polymers investigated there exist two families of  $\text{CH}_3$  groups moving with very different rates.<sup>5,6</sup> In what follows this model will be referred to as the simple rotational model (SRM). When the QENS spectra were fitted by means of this model, an anomalous non-Arrhenius behavior of the corresponding jumping rates was deduced. Another peculiar result obtained when the SRM is applied to polymers is that different spectrometers (different energy resolution) give rise to different rotation rates at the same temperature. In spite of the several explanations proposed<sup>4</sup> concerning these peculiar results, they are still open to controversy.

In order to contribute to these open questions, in the work reported in this paper, we have investigated the  $\text{CH}_3$  dynamics in poly(vinyl methyl ether) (PVME) by means of time-of-flight (TOF) neutron scattering techniques. The experimental spectra obtained can be described by the SRM although, like in other polymers,<sup>4</sup> the values of the model parameters found display an anomalous behavior. In this work, we have also developed a more general and realistic model for the  $\text{CH}_3$  dynamics. In this new approach, we have considered that, due to the amorphous character of the system investigated, the  $\text{CH}_3$  groups feel different local environments which can be supposed as randomly distributed. Therefore, we have considered the rotation of all the methyl groups with different rates instead of assuming only two kinds of methyl groups. A random distribution of the jumping rates has been postulated. We will show that, when this general model is applied to PVME, the experimental behavior can be perfectly described and, in addition, the anomalous behavior of the model parameters vanishes.

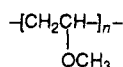
The outline of this paper is as follows: In section 2 the experimental details are presented. The results obtained are depicted in section 3. A discussion of the results obtained in the framework of the two models considered

\* Abstract published in *Advance ACS Abstracts*, May 1, 1994.

is shown in section 4. The conclusions of this work are reported in section 5.

## 2. Experimental Section

A protonated PVME sample from Polysciences Inc. with average molecular weights  $\bar{M}_n = 37\,000$  and  $\bar{M}_w = 63\,000$  and with a chemical formula of the repeating unit of



was purified using benzene as solvent and *n*-hexane as precipitant agent. Films for neutron measurements were made by casting from adequate solutions in PVME and dried under vacuum at a temperature of 60 °C for several days. The absence of residual of solvent in the dried samples was monitored by both nuclear magnetic resonance and Fourier transform infrared spectroscopy. The glass transition temperature measured by differential scanning calorimetry (DSC) at a heating rate of 10 K/min was 250 K. This value corresponds to the midpoint temperature of the specific heat step at constant pressure where a clear change is observed.

The neutron scattering experiments were performed on the IN6 time-of-flight (TOF) spectrometer at the Institut Laue Langevin (ILL, Grenoble, France) with an incident wavelength of 5.1 Å giving an energy resolution of 0.07 meV. Several measurements were carried out below and above the glass transition in the range of temperatures between 2 and 380 K.

The sample (thickness 0.07 mm) filled in an Al container yielded to a transmission of about 92%, which allows us to neglect the multiple scattering processes. The spectra were corrected for detector efficiency, sample container, absorption, and self-shielding with the standard ILL programs, and the cross section data were converted into dynamic factors,  $S(\theta, \omega)$ , where  $\hbar\omega$  and  $\theta$  are the energy exchange and the scattering angle, respectively. The constant angle  $S(\theta, \omega)$  was converted into constant- $Q$ ,  $S(Q, \omega)$ , by interpolation with the Ingrid code,<sup>7</sup>  $Q$  being the modulus of the momentum transfer. The actual  $Q$  range accessible after this procedure was between 0.7 and 1.7 Å<sup>-1</sup>.

For this kind of protonated system, the  $S(Q, \omega)$  laws mainly contain information on the geometry and the dynamics of the protons, due to their high incoherent scattering cross section (the ratio between the incoherent cross section  $\sigma_i$  and the total scattering one  $\sigma_s$  is about  $\sigma_i/\sigma_s = 0.96$ ). Therefore, it can be considered to a good approximation that the  $S(Q, \omega)$  scattering law could be represented only by its incoherent part.

## 3. Results

In addition to vibrational contributions, in the temperature range below the glass transition temperature  $T_g$ , the side group motion will be the main process responsible for the features appearing in the neutron spectra, either in the quasi-elastic domain or in the inelastic region. Main-chain motions or large conformational rearrangements can be considered to be frozen-in below and at  $T_g$  and would contribute only to the elastic intensity of the spectra. As commented on above, two types of methyl dynamics have been reported for polymers: torsional motions which mainly give rise to inelastic peaks around 25 meV and diffusional rotations of these groups which are mainly revealed in the quasi-elastic (QE) region.

In order to show the temperature range where the side group dynamics might be detected by IN6, the logarithm of the elastic peak intensity obtained directly from the raw data has been plotted in Figure 1 versus temperature. In this plot the intensity has been normalized to the scattering intensity at 2 K where it can be supposed that the system is completely frozen and therefore the observed intensity is purely elastic. In Figure 1 we found that, as expected, the elastic intensity decreases continuously with temperature and shows the following features: a linear behavior of  $\log(I)$  which is present up to about 100 K, a

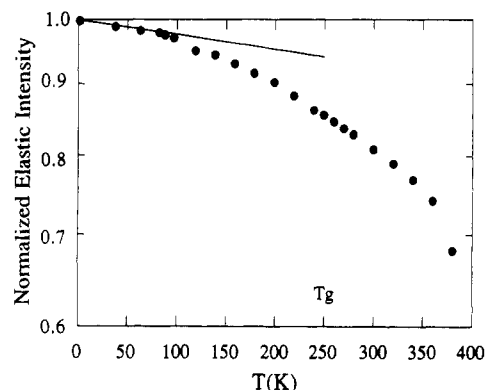


**Figure 1.** Temperature dependence of the normalized elastic intensity of PVME at a momentum transfer  $Q = 1.6 \text{ Å}^{-1}$ .

faster nonlinear decrease of  $\log(I)$  between 100 and 300 K, and finally an additional decrease above 300 K. The low-temperature linear behavior can be explained in the frame of the harmonic approximation where the vibrational mean-square displacement increases linearly with the temperature and therefore induces a linear decrease of the logarithm of the elastic intensity through the Debye-Waller factor (DWF)  $\exp[-1/3 \langle u^2 \rangle Q^2]$ ,  $\langle u^2 \rangle$  being the mean-squared displacement. The faster nonlinear decrease of  $\log(I)$  in the range of temperature between 100 and 300 K could be attributed to some motions other than vibration which start to be detected in the IN6 time range, and therefore the number of "elastically" scattered neutrons is faster reduced. For PVME the methyl group dynamics should be responsible for this behavior. On the other hand, the additional extra decrease of  $\log(I)$  occurring some degrees above 300 K ( $T_g + 50\text{K}$ ) could be an indication that the main-chain segmental dynamics starts to appear clearly in the IN6 time window.

As mentioned above, the decrease of the elastic intensity of the neutron spectra in the temperature range from 100 to 300 K should be associated with the methyl group dynamics. The extra decrease of the elastic intensity should have the corresponding counterpart in the inelastic range or in the quasi-elastic part of the spectra. Opposite to other side group polymeric systems,<sup>4</sup> where a peak observed in the inelastic neutron spectra at about 200 cm<sup>-1</sup> ( $\approx 25 \text{ meV}$ ) was attributed to the CH<sub>3</sub> torsion, no peak in the inelastic region (from 1 to 50 meV) of the PVME IN6 spectra was detected. However, a clear quasi-elastic broadening is observed in the temperature range above 120 K. This behavior is in agreement with the expected very low energy barrier corresponding to the ester methyl group diffusional rotation. Figure 2a shows constant- $Q$  spectra at different temperatures. In this figure the corresponding experimental resolution has been included in order to show the broadening of the elastic line. A similar broadening is observed in Figure 2b where spectra corresponding to different momentum transfers at constant temperature are also presented. Since, as mentioned above no peak in the inelastic region of the spectra was observed, the methyl group motion should mainly correspond to a rotation.

Taking into account that in PVME the CH<sub>3</sub> dynamics is mainly observed as a broadening of the elastic line, we will refer in what follows to the quasi-elastic (QE) range, from -2 to +2 meV, of the experimental spectra. Assuming that the vibrations of the protons around their average position and their motion other than vibration are uncoupled, it can be shown that in the QE region the vibrational contribution to the QE scattering is only through a Debye-Waller factor. In addition, for tem-

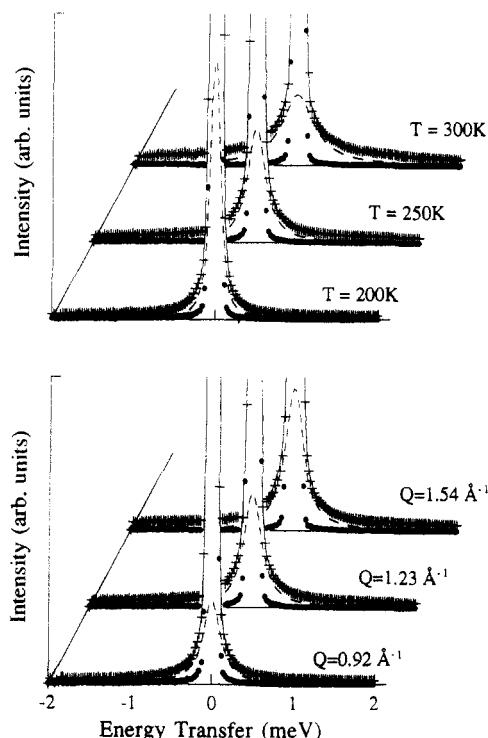


**Figure 2.** Constant  $S(Q, \omega)$  spectra for: (top) different temperatures at  $Q = 1.23 \text{ \AA}^{-1}$ ; (bottom) different momentum transfers at  $T = 250 \text{ K}$ . The resolution function ( $\bullet$ ), the fitted Lorentzian function (dashed line), and the total fitting function (solid line) are also shown.

peratures below and even around  $T_g$ , the main-chain protons could be considered as frozen in the IN6 window and should contribute to the incoherent dynamical structure factor in the QE range  $S^{QE}(Q, \omega)$  only as an elastic peak. In these conditions  $S^{QE}(Q, \omega)$  is given by:

$$S^{QE}(Q, \omega) = F(Q) \left\{ \frac{1}{2} \delta(\omega) + \frac{1}{2} S^M(Q, \omega) \right\} + B(Q) \quad (1)$$

where  $F(Q)$ , which includes the DWF term, is a factor to scale the model and the experimental intensities,  $S^M(Q, \omega)$  is the incoherent dynamical structure factor associated with the methyl group motion, and  $B(Q)$  is a flat background which would account for any possible fast contribution not considered in the model function and/or some residual instrumental background contribution. The factors  $1/2$  in eq 1 come from the fact that in each monomeric unit of PVME there are three fixed main-chain protons and three methyl protons. In the next section two models will be considered and therefore two different expressions of  $S^M(Q, \omega)$  will be given.

## 4. Discussion

**4.1. Simple Rotation Model.** In this section we consider the SRM to describe the methyl rotation dynamics in PVME. In this framework the experimental QENS spectra can be fitted by means of eq 1 considering the following model function:

$$S^M(Q, \omega) = A(Q) \delta(\omega) + [1 - A(Q)] L(\omega) \quad (2a)$$

with

$$L(\omega) = \frac{1}{\pi} \frac{h}{h^2 + \omega^2} \quad (2b)$$

convoluted with the experimental resolution. In eq 2a,  $A(Q)$  represents an empirical elastic incoherent structure

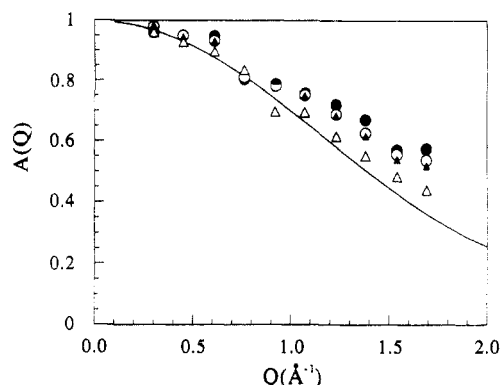


**Figure 3.** Experimental  $A(Q)$  behavior at different temperatures: ( $\bullet$ ) 160 K, ( $\circ$ ) 200 K, ( $\blacktriangle$ ) 240 K, and ( $\triangle$ ) 280 K. The solid line is the theoretical  $A_0(Q)$ .

factor which would correspond to the methyl group motion and contains all the information relative to the geometry of the motion. On the other hand, the half-width at half-maximum (hwhm)  $h$  of the Lorentzian function  $L(\omega)$  gives insight into the dynamics of the proton motion, i.e., the jumping rate of the methyl group protons. Thus, the fitting parameters of this model were the amplitude of the elastic contribution associated with the  $\text{CH}_3$  groups  $A(Q)$ , the hwhm of the Lorentzian function  $L(\omega)$ , and the flat background  $B(Q)$ . Good fits were obtained in the temperature range  $T \leq 300 \text{ K}$ . Above 300 K it appears that the dynamics of the main chain starts to influence the shape of the QENS spectra.<sup>8</sup> In the framework of the above-mentioned model it was expected that, if all the  $\text{CH}_3$  groups perform rotational jumps over three positions around the O- $\text{CH}_3$  bond, the  $Q$  dependence of the EISF corresponding to the methyl group motion would be given by the following law:<sup>2</sup>

$$A_0(Q) = \frac{1 + 2j_0(Qr_{\text{H-H}})}{3} \quad (3)$$

In eq 3  $j_0$  is the zeroth-order spherical Bessel function and  $r_{\text{H-H}}$  is the hydrogen-hydrogen distance in the  $\text{CH}_3$  group which has been estimated to be about  $1.78 \text{ \AA}$ .<sup>6</sup> When eq 3 was compared with the  $A(Q)$  values obtained from the fitting procedure, systematic deviations were found in the  $T$  range investigated (Figure 3). A clear extra elastic component, which increases when the temperature is lowered, was found. As mentioned above, similar deviations have also been reported in the literature when this kind of model has been applied to the description of the ester  $\text{CH}_3$  side group dynamics of poly(methyl methacrylate) (PMMA).<sup>4,6</sup> In order to avoid the discrepancy between the model  $A_0(Q)$  and the actually obtained  $A(Q)$  behavior, it can be assumed that only a fraction  $p \approx [1 - A(Q)]/[1 - A_0(Q)]$  of the  $\text{CH}_3$  groups in the sample is able to perform the rotational hopping while the remaining  $\text{CH}_3$  groups are frozen or at least move so slowly that they cannot be detected in the IN6 spectra.<sup>5,6</sup> By means of this assumption we have been able to describe the experimental behavior and to obtain the temperature evolution of the magnitudes characteristic of the methyl group dynamics, namely,  $p$  and  $h$ , which were found to be nearly  $Q$ -independent as expected. In addition, we have also evaluated the temperature behavior of  $B(Q)$ . The behavior obtained for these fitting parameters is shown in Figure 4. The results obtained could be summarized as follows:

(i) The fraction of methyl groups participating in the rotation process is found to increase with temperature below and above the glass transition temperature. However, the slope of  $p(T)$  increases markedly above  $T_g$ .

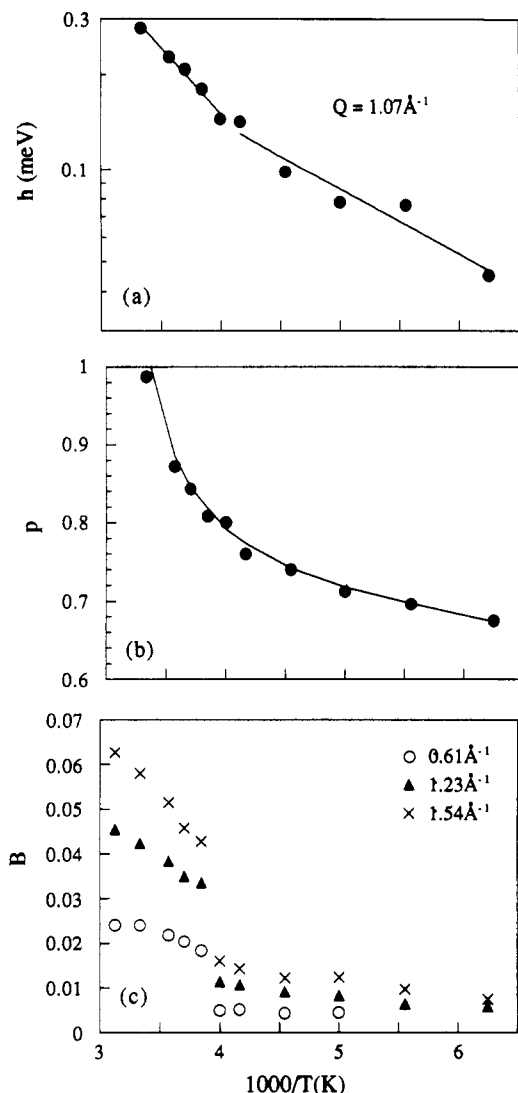


**Figure 4.** Temperature behavior of the parameters extracted using the simple rotation model SRM: (a) the half-width at half-maximum of the Lorentzian function contributing to the quasi-elastic experimental broadening of the spectra; (b) the fraction of moving  $\text{CH}_3$  groups; (c) the background.

(ii) The temperature behavior of  $h$  is not well described by a single Arrhenius law, but the apparent activation energy seems to increase with temperature.

(iii) The background, which increases linearly with  $Q$ , shows a significant increment just at  $T_g$ . The origin of this background is not clear, but it could include phonon-like low-frequency excitations and its increase in the  $T_g$  range could be associated with the appearance of the fast dynamical process which seems to be general for glass-forming materials.<sup>9,10</sup>

From these results it appears that the  $\text{CH}_3$  dynamics in PVME shows similar behaviors to the ones reported for the ester side group in PMMA. However, it seems that the glass transition process affects strongly the fast dynamics of the  $\text{CH}_3$  side group. Moreover, several questions remain unsolved in the application of this model.

(i) The model had to consider two different families of methyls: the frozen ones and the methyls moving uniformly. This situation implies a bimodal distribution of rotation rates whose physical origin is difficult to understand.

(ii) The physical interpretation of the increase of the activation energy as the sample temperature passes through  $T_g$  is not clear. Another related question is how

the increase of the fitting background in the  $T_g$  range can influence the temperature change of the other quantities.

All of these anomalies have led us to consider a different approach which seems to be more realistic.

**4.2. Rotation Rate Distribution Model.** A more realistic physical picture for the methyl group dynamics could be given by the rotation of all the methyl groups with different rates. In fact, it seems realistic to consider that, in amorphous polymers, the methyl groups in the system are present in different local environments. The origin of such different local environments should be attributed to both the lack of regularity of the main-chain conformation and/or the structural disorder characteristic of any glassy system. These different local environments should produce an energy landscape in the configurational space.<sup>11</sup> As a consequence, a distribution of the jumping rates for the methyl group rotational hopping should be expected on the basis of the Arrhenius law:

$$h(T) = h_\infty \exp(-E/RT) \quad (4)$$

where  $h_\infty$  is related to the attempt frequency,  $R$  is the gas constant, and  $E$  is the activation energy for the methyl rotation that measures the height of the barrier between equivalent positions.

In the proposed model we have considered a distribution of jumping rates whose origin can be either the distribution of the activation energies or the distribution of the attempt frequencies or both. The  $S^M(Q, \omega)$  model function is then given by:

$$S^M(Q, \omega) = A_0(Q) \delta(\omega) + [1 - A_0(Q)] \sum_{j=1}^N [g_j L_j(\omega)], \quad \text{with } \sum_{i=1}^N g_i = 1 \quad (5)$$

where  $A_0(Q)$  is given by eq 3 and  $L_i(\omega)$  are Lorentzian functions with a hwhm  $h_i$  and weight  $g_i$ . This rotation rate distribution model (RRDM) can be considered as a generalization of the SRM previously described. The SRM model with a fraction  $p$  of mobile methyls is recovered with  $N = 2$ ,  $g_1 = p$ ,  $h_1 = h$ , and  $h_2 \approx 0$ .

As a model function of the jumping rates distribution, a log-Gaussian function has been assumed, taking into account the randomness inherent to the  $\text{CH}_3$  environments. Thus,  $g_i$  has been evaluated as:

$$g_i \propto g(\ln h_i) = \frac{1}{\sigma(2\pi)^{1/2}} \exp\left[-\frac{1}{2\sigma^2} \ln^2\left(\frac{h_i}{h_0}\right)\right] \quad (6)$$

where the proportionality constant has been taken to ensure the condition  $\sum_{i=1}^N g_i = 1$ . In eq 6,  $\sigma$  is the variance of the Gaussian distribution and  $h_0$  is the hwhm of the more probable Lorentzian component. The values of  $h_i$  have been chosen equally spaced in the logarithmic scale in a range wide enough to cover the whole interval where eq 6 provides significant values of  $g_i$ . We have used 20 Lorentzian functions, and we have tested that following the above-mentioned procedure the results obtained were not significantly modified when a higher number of Lorentzian functions were considered.

In these conditions the calculated  $S^{\text{QE}}(Q, \omega)$  was convoluted with the experimental resolution and a least-squares fitting procedure was performed. Two steps were followed. The spectra were first refined individually, and in this case the model function was specified by four adjustable parameters:  $\sigma$ ,  $h_0$ ,  $F(Q)$ , and  $B(Q)$ . Good fits were obtained in the temperature range  $180 \text{ K} \leq T \leq 300 \text{ K}$  (see Figure 2), and the resulting values of  $h_0$  as well as

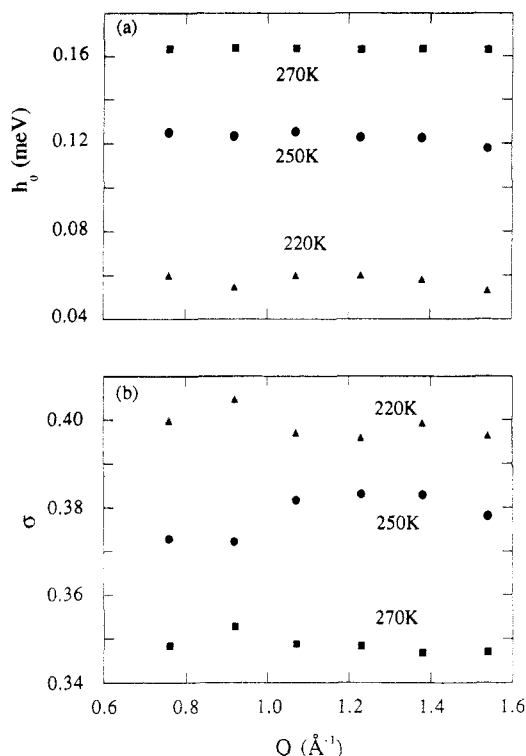


**Figure 5.**  $Q$  dependence of the  $h_0$  and  $\sigma$  parameters involved in the rotation rate distribution model.

$\sigma$  were found to be nonsystematically  $Q$ -dependent (see Figure 5). The fact that  $h_0$  is  $Q$ -independent confirms the result already obtained with the SRM, indicating that we are dealing with a localized motion. Afterward, the  $h_0$  and  $\sigma$  values have been chosen at each of the studied temperatures by averaging the values obtained at the different  $Q$ 's considered in the first step. In a second step, these values were fixed and the fitting procedure was refined in order to obtain the  $B(Q)$  and  $F(Q)$  behaviors at the different temperatures investigated. The fitting curves obtained after this second step are undistinguishable from the ones obtained in the first step.

For temperatures higher than 300 K, the fits with the RRDM are not so good and it seems necessary to take into account some other process that might appear in the IN6 energy window. In fact, from measurements on the high-resolution spectrometers (IN10 and IN13 at the Institut Laue Langevin, Grenoble, France) it appears that the dynamics of the  $\alpha$ -relaxation contributes to the dynamical structure factor for temperatures above 300 K.<sup>8</sup> Therefore, we will focus our attention on the temperature range  $T \leq 300$  K. The study of the high-temperature region  $T > 300$  K will be the subject of a future work.

Once we have shown that the broadening of the QENS spectra can be described by means of the RRDM for the  $\text{CH}_3$  rotation, we can study the temperature dependence of the parameters characterizing this dynamical process. The temperature behavior of  $h_0$  and  $\sigma$  is displayed in Figure 6. As can be seen in Figure 6a,  $h_0$  follows an Arrhenius law (eq 4). Notice that the Arrhenius behavior extends over the whole temperature range investigated and it is not influenced by the glass transition process, contrary to the behavior deduced by means of the SRM (see Figure 4a). This finding is also very different from the clear non-Arrhenius behavior of the methyl group in PMMA<sup>4,6</sup> obtained through the SRM. Therefore, it can be concluded at this stage that the anomalous temperature dependence found for PVME in the framework of the SRM is a consequence of neglecting the jumping rate distribution

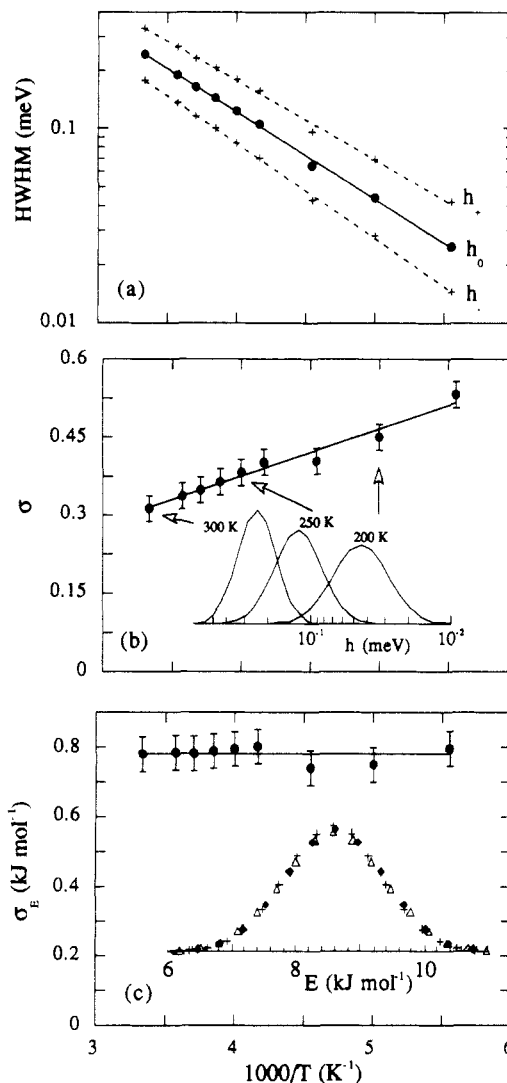


**Figure 6.** Temperature dependence of the parameters characterizing the side group dynamics extracted using the RRDM. The inset of Figure 6b shows the jumping rate distribution function at the temperatures indicated. The inset in Figure 6c shows the corresponding activation energy distributions at (♦) 200, (Δ) 250, and (+) 300 K.

in the corresponding model function. In the framework of the RRDM the rotation of  $\text{CH}_3$  groups can be seen as a simple activated process. From the fitting of the experimental behavior of  $h_0(T)$  shown in Figure 6a, an activation energy of about  $8.4 \text{ kJ mol}^{-1}$  is deduced by means of eq 4. Such a value is in the range expected for this kind of side group rotation in polymeric systems<sup>12</sup> and is clearly higher than that obtained previously with the SRM. On the other hand, the value of  $h_{\infty} = 3.1 \times 10^{12} \text{ s}^{-1}$  obtained in the Arrhenius fitting is, as it should be, on the order of the Debye frequency. From this fitting, we obtain  $h_0(T_g) = 1.8 \times 10^{11} \text{ s}^{-1}$  which, once converted into mobility time,<sup>2</sup> gives an average characteristic time at  $T_g$  of  $\tau_0(T_g) = 3/h_0(T_g) = 16.5 \text{ ps}$ . This low value is in agreement with the decoupling between the methyl group fast dynamics and the slow main-chain dynamics associated with the  $\alpha$ -relaxation ( $\tau \approx 1 \text{ s}$  at  $T_g$ ).

Another parameter of crucial interest in the framework of the model considered here is  $\sigma$  which measures the width of the distribution of jumping rates. In Figure 6a, in addition to  $h_0(T)$ , the temperature behavior of  $h_+$  and  $h_-$  is shown. The  $h_+$  and  $h_-$  values have been defined as  $h_0 \exp(\sigma)$  and  $h_0 \exp(-\sigma)$ , respectively, and correspond to the standard deviation of the distribution function. From Figure 6a it is clear that the distribution of jumping rates

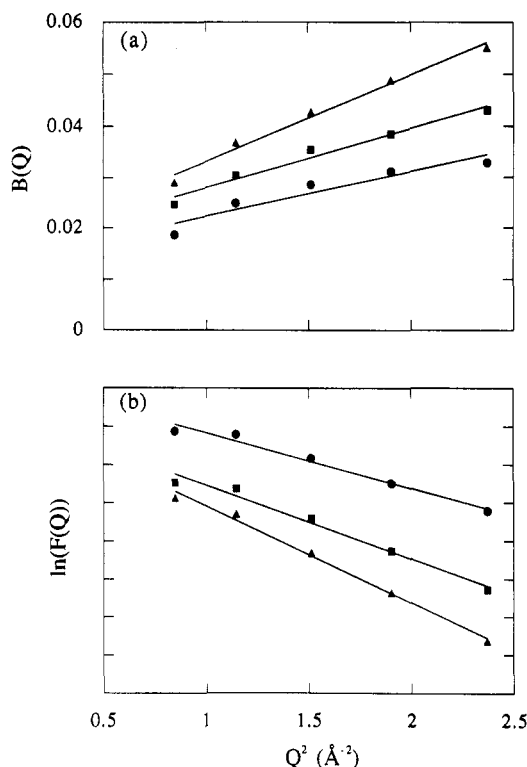


**Figure 7.**  $Q$  dependence of the background (a) and of the amplitude factor (b) obtained from the RRDM model at three different temperatures: (●) 200 K, (■) 250 K, and (▲) 280 K.

narrows as  $T$  increases. Figure 6b shows that, accordingly,  $\sigma$  decreases continuously with temperature. The fitting of  $h_-(T)$  and  $h_+(T)$  by means of eq 4 leads to the values  $h_{\infty-} = 2.8 \times 10^{12} \text{ s}^{-1}$  and  $h_{\infty+} = 3.3 \times 10^{12} \text{ s}^{-1}$ , respectively, which within 10% are comparable to  $h_{\infty 0}$ . This fact is an indication that a distribution of activation energies is the main process responsible for the distribution of jumping rates observed. Assuming a constant value of  $h_{\infty i} = h_{\infty}$ , from eq 4 it is easy to see that the relationship between the distribution of jumping rates and the corresponding distribution of activation energies is given by:

$$g[\ln(h/h_{\infty})] = g(E/RT) \quad (7)$$

Thus, eq 6 can be rewritten as:

$$g_i \propto \exp\left[-\frac{1}{2\sigma^2} \ln^2\left(\frac{h_i}{h_0}\right)\right] = \exp\left[-\frac{1}{2\sigma^2} \left(\frac{E_i - E_0}{RT}\right)^2\right] = \exp\left[-\frac{1}{2\sigma_E^2} (E_i - E_0)^2\right] \quad (8)$$

$\sigma_E = \sigma RT$  being the width of the distribution of activation energies. Figure 6c shows the values of  $\sigma_E$  so obtained and the corresponding energy distribution. It is clear that, within the experimental uncertainty, the energy distribution remains constant with temperature. Error bars in Figure 6 were calculated, taking into account the scattering of  $\sigma(Q)$  data (see Figure 5b). Therefore, it can be concluded that the energy landscape that the  $\text{CH}_3$  groups feel remains unaltered in the temperature range investigated.

Once the methyl group dynamics have been described in the framework of the RRDM we will briefly discuss in the following the  $Q$  and  $T$  dependence of the  $B(Q)$  and  $F(Q)$  parameters obtained in the fitting procedure. These parameters should include in principle all the information concerning motions other than the methyl group rotation. Figure 7 shows the behavior of  $B(Q)$  and  $F(Q)$  at some of

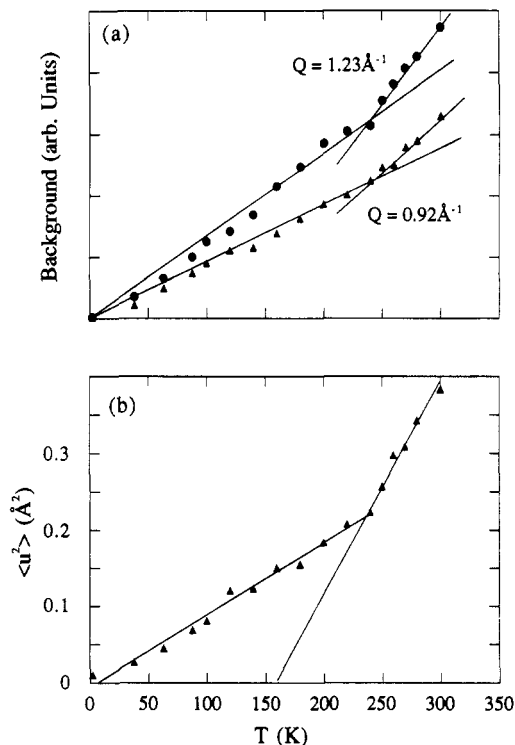


**Figure 8.** Temperature dependence of (a) the background at two different momentum transfers and (b) the mean-square displacement.

the investigated temperatures. In Figure 7a, a clear linear increase of the background  $B(Q)$  with  $Q^2$  is observed. This behavior suggests a vibrational-like origin for this background. On the other hand, as above commented,  $F(Q)$  includes a decrease of the intensity associated with the harmonic vibrations which would be described by means of the DWF. In Figure 7b the fitting of the experimental values of  $F(Q)$  to a DWF decay is shown. In the whole temperature range the fitting is quite good and the different values of  $\langle u^2 \rangle$  can be calculated as a function of temperature. As is shown in Figure 8b, a linear increase of  $\langle u^2 \rangle$  with temperature up to about 240 K is found. This proportionality with temperature observed below the glass transition temperature corresponds to what it is expected for a harmonic oscillator in the Debye approximation. Above 250 K  $\langle u^2 \rangle$  is still linear with temperature but increases more rapidly. This is a common experimental feature of glassy main-chain polymers (e.g., polybutadiene (PB)<sup>13</sup> and polyisobutylene (PIB)<sup>14</sup> as well as of low molecular weight glass-forming liquids like *o*-terphenyl<sup>15</sup> and selenium.<sup>16</sup> As shown in Figure 8a,b this extra increase of  $\langle u^2 \rangle$  is clearly correlated with the extra  $T$  increase of the background around  $T_g$ .

## 5. Conclusions

QENS results on PVME in the time range  $10^{-11}$ – $10^{-13}$  s confirm the assignment of the methyl group proton rotation as the motion responsible for the QE broadening in the IN6 neutron scattering experiments. Considering a 3-fold rotational hopping of the methyl side group protons, we have shown that the peculiar behaviors observed by using the SRM disappear when a more realistic and general model consisting of a distribution of the jumping rates is considered. This model takes into account the inhomogeneity of the methyl dynamics due to the presence of different local environments which is at the origin of a jumping rates distribution. Assuming a log-Gaussian distribution of jumping rates, we find that each jumping rate follows a simple Arrhenius-type law. A

Gaussian distribution of the energy barriers for the CH<sub>3</sub> rotation which remains almost constant with temperature was found to be the origin of this distribution of jumping rates. A mean value of the activation energy of about 8.4 kJ mol<sup>-1</sup> was deduced with a 10% standard deviation.

One point not resolved yet is how this model can be extrapolated and convoluted with the main-chain segmental dynamics to account for the experimental spectra well above  $T_g$  ( $T > 300$  K). This work is now in progress and will be the subject of a separate publication. Finally, it seems reasonable to think that the RRDM could be applied to the previous measurements about the ester CH<sub>3</sub> dynamics in other polymeric systems in order to check if the peculiar results obtained by means of the SRM also disappear when the model proposed here is considered.

**Acknowledgment.** We thank Guipuzkoako Foru Al-  
dundia and Iberdrola S. A. for partial financial support.  
A.C. acknowledges a grant from the Basque Government.  
We also thank Dr. B. Frick and ILL for experimental  
neutron facilities.

## References and Notes

- (1) Bailey, R. T.; North, A. M.; Pethrick, R. A. *Molecular Motion in High Polymers*; Clarendon Press: Oxford, U.K., 1981.
- (2) Bée, M. *Quasielastic Neutron Scattering: Principles and Applications in Solid State Chemistry, Biology and Materials Sciences*; Adam Hilger: Bristol, U.K., 1988.
- (3) Higgins, J. S.; Allen, G.; Brier, P. N. *Polymer* **1972**, *13*, 157.
- (4) Gabrys, B.; Higgins, J. S.; Ma, K. T.; Roots, J. E. *Macromolecules* **1984**, *17*, 560.
- (5) Chahid, A.; Colmenero, J.; Alegría, A. *Physica A* **1993**, *201*, 101.
- (6) Floudas, G.; Higgins, J. S. *Polymer* **1992**, *33*, 4121.
- (7) Rieutord, F. private communication.
- (8) Colmenero, J.; Alegría, A.; Alberdi, J. M.; Alvarez, F.; Frick, B. *Phys. Rev.* **1991**, *B44*, 7321.
- (9) *Dynamics of Disordered Materials*; Richter, D., Dianoux, A. J., Petry, W., Teixeira, J., Eds.; Springer-Verlag: Berlin, 1989.
- (10) Colmenero, J.; Arbe, A.; Alegría, A. *Phys. Rev. Lett.* **1993**, *71*, 2603.
- (11) Angell, C. A. *Annu. Rev. Phys. Chem.* **1992**, *43*, 693.
- (12) Allen, G.; Wright, C. J.; Higgins, J. S. *Polymer* **1974**, *15*, 319.
- (13) Frick, B.; Richter, D.; Petry, W.; Buchenau, U. *Z. Phys.* **1988**, *B70*, 73.
- (14) Frick, B.; Richter, D. *Phys. Rev. B* **1993**, *47*, 14795.
- (15) Petry, W.; Bartch, E.; Fujara, F.; Kievel, M.; Sillescu, H.; Farago, B. *Z. Phys.* **1991**, *B83*, 175.
- (16) Buchenau, U.; Zorn, R. *Europhys. Lett.* **1992**, *18*, 523.